Scientia Iranica C (2017) 24(6), 3053–3063

Sharif University of Technology
Scientia Iranica
Transactions C: Chemistry and Chemical Engineering
www.scientiairanica.com

Investigating the viscoelastic fluid behavior in hollow fiber membrane fabrication process using Giesekus' model

H. Didari[a], M. Salami Hosseini[b,c,*] and R. Yegani[a]

a. *Department of Chemical Engineering, Sahand University of Technology, Sahand New Town, Tabriz, Iran.*
b. *Department of Polymer Engineering, Sahand University of Technology Campus, Sahand New Town, Tabriz, P.O. Box 53318/11111, Iran.*
c. *Institute of Polymeric Materials, Sahand University of Technology, Sahand New Town, Tabriz, Iran.*

Received 4 December 2016; received in revised form 12 April 2017; accepted 29 July 2017

KEYWORDS
Extrudate swell;
Finite-element method;
Giesekus' model;
Hollow fiber membrane;
Viscoelastic fluid.

Abstract. In the present study, attempts are made to study the behavior of a viscoelastic fluid in the hollow fiber membrane production process. For this purpose, the fluid is considered to obey the Giesekus' model and flow is taken as steady, two-dimensional and isothermal one. The flow field is obtained using DEVSS/SUPG scheme combined with a free surface tracking method. The obtained results are compared to the case of Newtonian fluid. It is shown that the extrudate swell is 20% more in the case of viscoelastic fluid. Moreover, the elastic behavior of the viscoelastic fluid significantly affects the velocity field in the extrudate outside the die. It causes the fluid flow to become reversed in the middle part of the extrudate as the direct result of the stress relaxation process, whereas such a behavior is not seen for Newtonian fluid. Also, the First Normal Stress Difference (FNSD) distribution in the extrudate is obtained and its variation is discussed. Furthermore, the effects of operational parameters, including die back pressure and take-up velocity, are investigated. Finally, the predicted extrudate swell for various operation conditions is compared to experimental results showing good agreement between experimental and simulated data.

1. Introduction

Membrane separation processes are widely used in a variety of industrial applications such as water-related technologies, medical applications, and gas separation processes. Among several conventional forms of the membranes, hollow fiber is the most preferred and suitable design of membrane due to its several advantages such as high surface area-to-volume ratio compared with other forms of membranes, such as flat sheet or spiral wound. So, using hollow fiber membrane results in high productivity, self-mechanical support, ease of operation and handling during module manufacturing, efficient cleaning procedures using vibration which is available only for hollow fiber membrane, and finally excellent mass transfer properties [1].

In the last decades, significant efforts have been made by membrane scientists to develop hollow fibers with desirable pore structures, thin selective layers, and elimination of dense skin layer. New hollow-fiber membranes were invented mostly based on the experience, empirical data, limited qualitative scientific findings, and luck. It is well documented that during hollow fiber membrane fabrication, there are many influential

*. *Corresponding author. Tel.: +98 41 3345 9082; Fax: +98 41 3344 4313*
E-mail address: salami@sut.ac.ir (M. Salami Hosseini)

doi: 10.24200/sci.2017.4490

variables that could drastically affect the conformation and performances of hollow fiber membranes [2]. Some variables can trigger a viscoelastic phenomenon such as die-swell, which is undesired since it may result in weak reproducibility of the permeation properties. Tanner [3] presented an elastic-fluid theory of die swell for long dies. He used the KBKZ constitutive equation. His results have good agreement with experiments. A work carried out by Pereira et al. [4] suggested that the die-swell can be avoided by increasing the solvent concentration in bore liquid and the distance spinneret precipitation bath even with high content of water in the bore liquid. It was also confirmed that a high viscosity of solution could minimize the die-swell effect. Wang and Lai [5] studied the effects of dope flow rate and flow angle within the spinneret during fabrication of hollow fiber membranes on the morphology, water permeability, and separation performance of polyethersulfone hollow fiber membranes. For this purpose, two spinnerets with different flow angles were designed and used. They concluded that higher dope flow rates inside the spinneret resulted in hollow fiber membranes with smaller pore sizes and denser skin layers due to the enhanced molecular orientation. Batchelor et al. [6] studied die swell experimentally on elastic liquid and Newtonian liquid of similar viscosity. The Reynolds number was about 10^{-8}. They showed that the die swell of elastic liquid increased with shear rate. Orbey and Dealy [7] studied experimentally the effects of die geometry and extrusion velocity on extrudate swell. They used four annular dies. They observed that 60 to 80 percent of the swell occurs in the first few seconds. They showed that the diameter and thickness swell depended strongly on die design.

As explained before, most of reported results were based on almost narrow practical efforts, and few data reported on the basis of combined numerical-experimental studies. Among few reports, therefore, some successful works could be referred to. Andrews [8] introduced a solution to the energy transfer where the motion equations were not taken into account. The attempt failed to predict the fiber-dimensional changes in the draw zone, and empirical estimation available from experimental studies was relied on. Ziabicki and Kedzierska [9] predicted the changes of the fiber dimensions using a simple force balance on the filament. Denn et al. [10] proposed a theoretical basis for modeling the melt/solid fiber spinning using approximate solutions of the conservation laws of energy and momentum. The resulted theoretical analysis was known as Thin Filament Analysis (TFA) based on the assumption of a high-aspect ratio of the fiber. Sano [11] and Guo and McHugh [12] coupled TFA with 2D mass transfer analysis and obtained concentration profiles at radial direction. They also provided a reference point for comparison and validation of the techniques developed as a part of the dissertation performed by Didari [13]. Berghmans et al. [14] performed simultaneous simulation for mass and heat transfers at the fiber outer surface where all physical parameters in the model were considered as constant. These models assumed that the filament moved at a constant velocity to avoid any solution to the moving equations. As the dope is a viscoelastic fluid, using viscoelastic model in the modeling and simulation of hollow fiber spinning process could result in more realistic results. Beris and Liu [15] used Upper-Convected Maxwell (UCM) model to simulate one-dimensional transient fiber spinning process and compared the results for the Newtonian and high Deborah number viscoelastic fluids. Lee et al. [16] used White-Metzner and Phan-Thien-Tanner viscoelastic models to investigate the effect of viscoelasticity on the draw resonance dynamics. They found that increasing elastic behavior of the fluid resulted in stabilizing melt spinning. Joo et al. [17] developed a numerical simulation for non-isothermal and two-dimensional melt spinning processes by considering Giesekus model. They solved governing equations using DEVSS-G/SUPG finite-element method. They found that the radially non-uniform stress profiles showed good agreement with experimental results for polyester resin. Behzadfar et al. [18] studied the effect of molecular structure and geometrical parameters on the extrudate swell phenomenon. They showed that extrudate swell changed nonlinearly with entrance angle, and that the molecular structure affected the extrudate swell significantly. Konaganti et al. [19] numerically studied the extrudate swell phenomenon using different viscoelastic constitutive equations. They found that integral models highly overpredicted the extrudate swell, whereas differential models slightly underpredicted the phenomenon. Konaganti et al. [20] studied the effect of damping function on extrudate swell. They studied the extrudate swell of an industrial-grade high-molecular-weight high-density polyethylene using the integral K-BKZ model. They performed simulation with different values of the Wagner exponent. The results showed that predictions are extremely sensitive to the Wagner damping function exponent. Konaganti et al. [21] studied the extrudate swell of industrial-grade high-molecular mass high-density polyethylenes in flat/slit dies using K-BKZ model. They showed that the integral K-BKZ model predicted well both the width and thickness extrudate swells. They demonstrated that extrudate swell measurements of the thickness swell were predominant in comparison with width swell.

The present study was carried out to cover the existing gap in 2D modeling of flow behavior to predict the extrudate swell and validate the model predictions with experimental data. In this study, the mathematical model of two-dimensional extrudate swell of

viscoelastic fluid was established using Giesekus' differential model. A stable solving method for the nonlinear problem was employed (DEVSS/SUPG) combined with a front tracking method proposed by Baaijens et al. and Soulaïmani et al. [22,23]. The investigation of 2D extrudate swell predicted by differential viscoelastic rheological model was successfully carried out and compared to experimental data.

2. Experimental

2.1. Materials

In the present study, linear low-density polyethylene (LLDPE), grade LL0209AA (MFI = 0.9 g/10 min, 190°C, 2.16 Kg), was purchased from Tabriz Petrochemical Company. Furthermore, liquid paraffin (density = 775 kg/m^3, Merck) and Irganox 1010 (Ciba Co.) were used as solvent and heat stabilizer, respectively.

2.2. Hollow fiber membrane preparations

Hollow fiber membranes were prepared by a batch-type indoor manufactured cylindrical machine. Measured amounts of LLDPE and mineral oil were fed into the cylinder; mixture was heated to above the melting point of LLDPE (140°C) while the solution was mixed continuously for 45 minutes. The polyethylene (PE) concentration was fixed at 20% wt. In order to prevent the degradation of PE, proper amount of antioxidant was added to the mixture. After preparing a homogeneous dope, the mixer was stopped to let the bubbles be released completely from the dope. Then, the homogeneous bubble free dope was fed into the spinneret by a gear pump under nitrogen atmosphere. The spinneret consists of outer and inner cylinders with diameters of 0.6 and 0.85 mm, respectively. The dope was introduced into the inner orifice at 160°C to make a lumen of the hollow fiber. The hollow fiber was extruded from the spinneret using various tank pressures to get different flow rates. In order to measure the extrudate swell of the extrudate, images were taken using a digital camera (SONY, DSC-H100-16.1) as hollow fiber came out of the spinneret. The images were analyzed using an open-source image analyzing software, Image J.

2.3. Rheological parameters of the dope

Small amplitude oscillatory measurements were carried out using 25 mm parallel plates on a stress-controlled rotational rheometer (Anton Paar, MCR 301) at 160°C. The linear viscoelastic parameters, including λ_i and G_i, were obtained by fitting the experimental data, using MATLAB's fitting toolbox, to the Maxwell model [24,25]:

$$G'(\omega) = \sum_i \frac{G_i \lambda_i^2 \omega^2}{1 + \lambda_i^2 \omega^2}, \tag{1}$$

Table 1. The Giesekus' model parameters at 160°C.

G_i (Pa.s)	λ_i (s)	α_i
15.2	0.01	0.016

$$G''(\omega) = \sum_i \frac{G_i \lambda_i \omega}{1 + \lambda_i^2 \omega^2}, \tag{2}$$

where $G'(\omega)$ is the storage modulus, $G''(\omega)$ is the loss modulus, and ω is the angular frequency. Using the obtained data and following the method proposed by Yesilata et al. [26], the anisotropy parameter (mobility factor) was obtained and shown in Table 1.

3. Mathematical modeling

The governing equations, continuity, and Navier-Stokes (NS) equations, for steady, laminar, isothermal and incompressible flow were considered as follows:

$$\boldsymbol{\nabla} \cdot \mathbf{u} = 0, \tag{3}$$

$$-\boldsymbol{\nabla} p + \boldsymbol{\nabla} \cdot (\tau) + \rho \mathbf{g} + \mathbf{f} = 0, \tag{4}$$

where ρ, $\mathbf{u}$, p, $\mathbf{g}$, τ, and $\mathbf{f}$ are the fluid density, velocity vector, pressure, gravitational acceleration, stress tensor, and applied external force vector, respectively. $\boldsymbol{\tau}$, the stress tensor, could be split into two parts:

$$\boldsymbol{\tau} = \boldsymbol{\tau}_\mathbf{s} + \boldsymbol{\tau}_\mathbf{p}, \tag{5}$$

where $\boldsymbol{\tau}_\mathbf{s}$ is the stress due to the viscous part, and $\boldsymbol{\tau}_\mathbf{p}$ is the excess stress due to the elastic part of the fluid behavior. $\boldsymbol{\tau}_\mathbf{s}$ could be calculated using Newton's method, $\boldsymbol{\tau}_\mathbf{s} = 2\ \mu \mathbf{D}$, where $\mathbf{D}$ is the deformation rate tensor:

$$D = \frac{1}{2}\left(\boldsymbol{\nabla}\mathbf{u} + \boldsymbol{\nabla}\mathbf{u}^\mathbf{T}\right), \tag{6}$$

where $\boldsymbol{\nabla}\mathbf{u}$ is the velocity gradient tensor. The one mode Giesekus model [27] was considered as the model of the excess stress and expressed as follows:

$$\boldsymbol{\tau}_\mathbf{p} + \lambda \boldsymbol{\tau}_\mathbf{p}^{\boldsymbol{\nabla}} + \alpha \frac{\lambda}{\eta_p}\{\boldsymbol{\tau}_\mathbf{p} \cdot \boldsymbol{\tau}_\mathbf{p}\} = 2\eta_p \mathbf{D}, \tag{7}$$

where $\boldsymbol{\tau}_\mathbf{p}^{\boldsymbol{\nabla}}$, λ, α, and η_p are the upper convected derivative of the excess stress tensor, relaxation time, anisotropy parameter (mobility factor), and zero shear viscosity of the fluid, respectively. The upper-convected derivative of the excess stress tensor is given by:

$$\boldsymbol{\tau}_\mathbf{p}^{\boldsymbol{\nabla}} = \frac{D}{Dt}\boldsymbol{\tau}_\mathbf{p} - [\boldsymbol{\nabla}\mathbf{u}^\mathbf{T} \cdot \boldsymbol{\tau}_\mathbf{p}] - [\boldsymbol{\tau}_\mathbf{p} \cdot \boldsymbol{\nabla}\mathbf{u}]. \tag{8}$$

Eqs. (3), (4), and (7) were solved together using DEVSS/SUPG method with a moving mesh consideration

to predict the extrudate swell phenomenon. Figure 1 shows the domain geometry and corresponding boundary conditions. The flow field was discretized into 34400 elements and 35301 nodes as shown in Figure 1 by the mapping mesh generation method. Since the geometry was axisymmetric, the two-dimensional cross-section was taken into account as representative of full three-dimensional geometry of the calculation domain. The geometry and boundary conditions of the die head are summarized in Table 2. Four cross-sections along the extruded were considered to compare the results, shown in Figure 2.

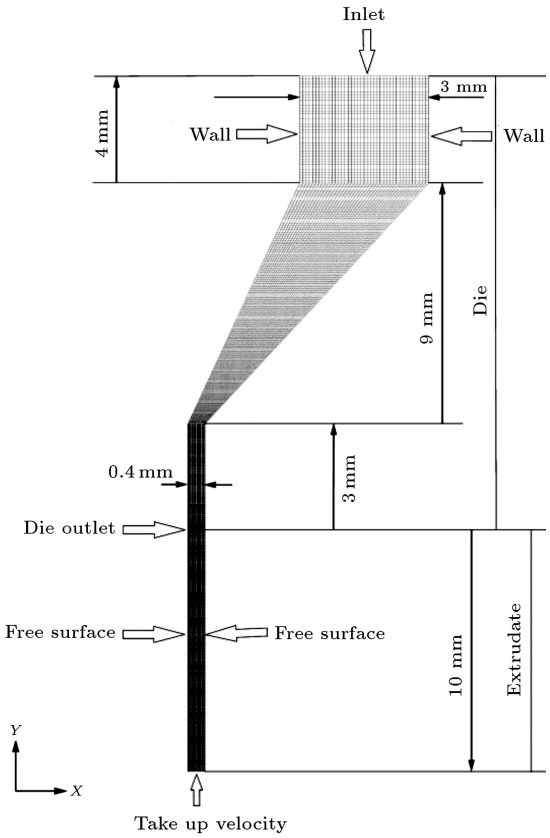

Figure 1. The domain geometry and corresponding boundary conditions.

Table 2. Boundary conditions in the die head.

Code	Inlet pressure (bar)	Take-up velocity (m/s)
P1r10	1	0.068 (10 rpm)
P1r20	1	0.136 (20 rpm)
P1r30	1	0.204 (30 rpm)
P1.5r20	1.5	0.136 (20 rpm)
P1.5r30	1.5	0.204 (30 rpm)
P1.5r40	1.5	0.272 (40 rpm)
P2r30	2	0.204 (30 rpm)
P2r40	2	0.272 (40 rpm)
P2r50	2	0.34 (50 rpm)

4. Result and discussion

4.1. Extrudate swell

Figure 3 depicts the extrudate profile and thickness for Newtonian and viscoelastic fluids. Figure 4 compares the extrudate swell of the extrudate in case of Newtonian and viscoelastic fluids. It could be seen that the extrudate swell for viscoelastic fluid was much

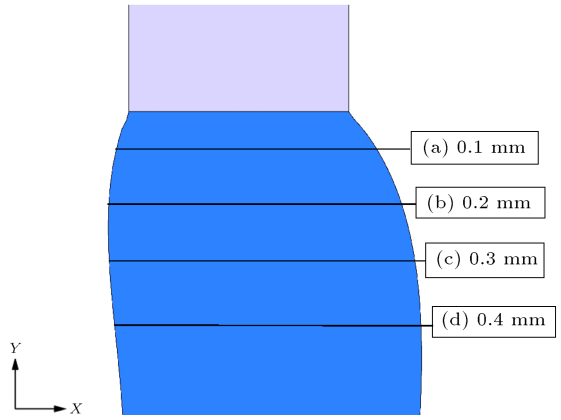

Figure 2. Location of cross-sections at extrudate.

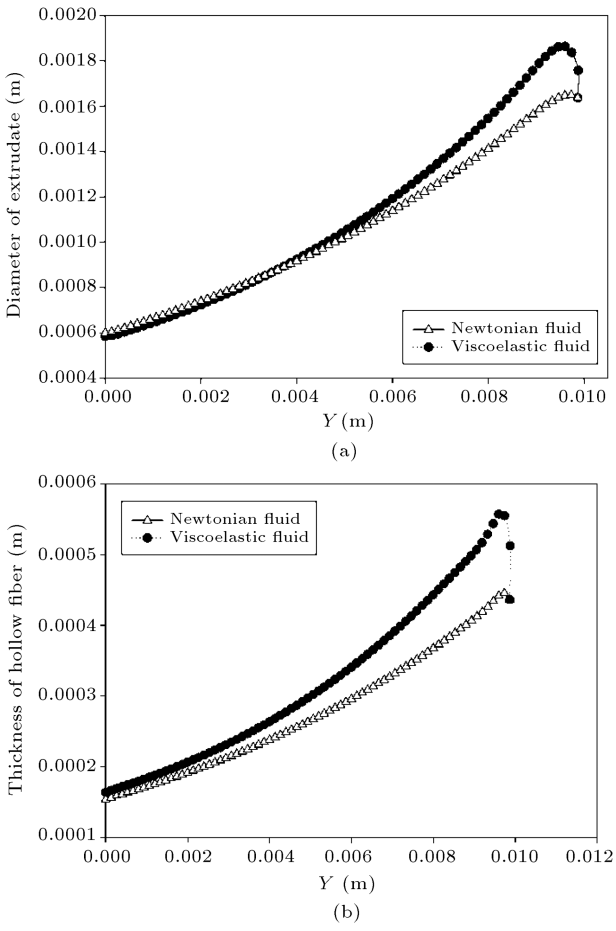

Figure 3. (a) The extrudate profile. (b) Thickness for Newtonian and viscoelastic fluids with the prescribed condition (P1.5r30).

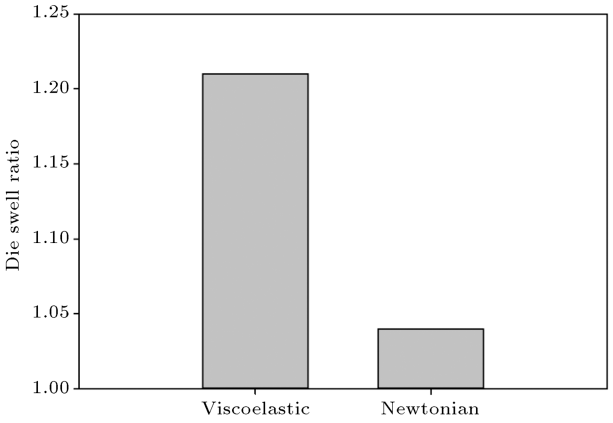

Figure 4. Comparing the die swell of the extrudate in the Newtonian and viscoelastic fluids.

greater than that for Newtonian one as expected. As the viscoelastic fluid came out of the die, the fluid was allowed to relax the stress stored due to elastic nature. During this relaxation process, the fluid shrunk back returned which caused the increase of extrudate width and lowering the axial velocity of the fluid in extrudate as mentioned before.

4.2. Effect of the fluid behavior

Figure 5 shows the velocity distribution in cross-sections (a) to (d) for the Newtonian fluid. It could be noted that as soon as the fluid comes out of the die, the velocity profile remains the same as that in the die. Only the velocity at the edge of the cross-section becomes different in comparison to the velocity profile of the die, which is the effect of no-slip condition of the wall. Since there was no wall at the edge of cross-section (a), the fluid of this part started to move with the extrudate and the velocity at this part increased. In this cross-section, the fluid located at the middle part had almost the same velocity as the one located in the middle part inside the die. It reflects the fact that, at this point, the flow was still under the influence of the fluid field within the die. As fluid moved out and reached cross-section (b), velocity profile started to level off and get closer to plug flow profile due to the wall removal. In cross-sections (c) and (d), the velocity distribution was almost uniform and plug-like, showing that the effect of flow field inside the die faded into insignificance. It could be explained that the Newtonian fluid has no memory, and previous states do not affect the present one, and the fluid is in its relaxed mode at every stage.

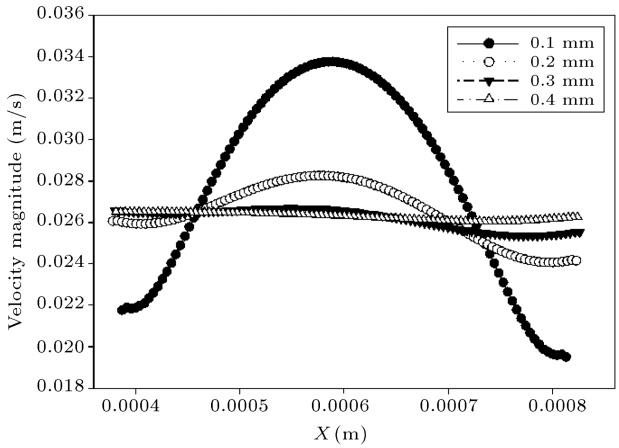

Figure 5. The velocity distribution in cross-sections (a) to (d) for the Newtonian fluid with the prescribed condition (P1.5r30).

The obtained results of viscoelastic material showed a different flow behavior in comparison to Newtonian fluid in the same condition (Figure 6). The velocity profile in the vicinity of the die outlet showed an up-turn pattern at the edge of the extrudate while there was not such a pattern in Newtonian fluid case (Figure 7). It is well known that viscoelastic fluid has memory due to elastic part of its behavior, and it could store the exerted stress inside the die and would try to relax and release the stored stress as soon as it came out of the die. Since the fluid inside the

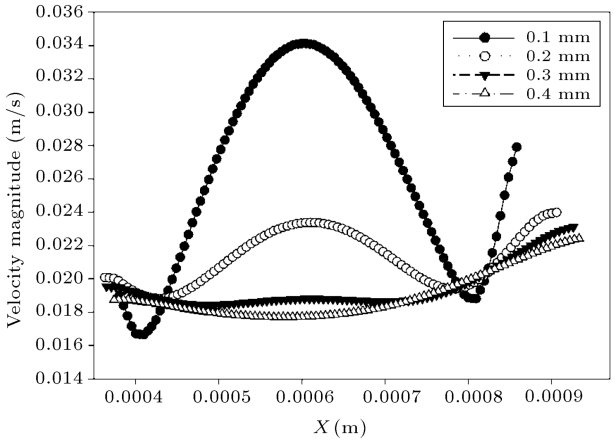

Figure 6. The velocity profile at different cross-sections of hollow fiber with the prescribed condition (P1.5r30).

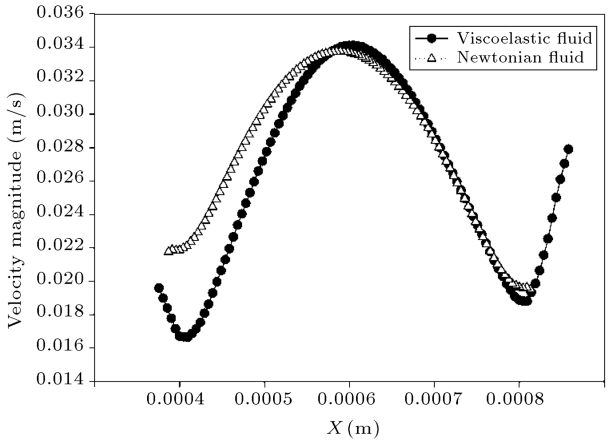

Figure 7. The velocity profile in the vicinity of the die outlet with the prescribed condition (P1.5r30).

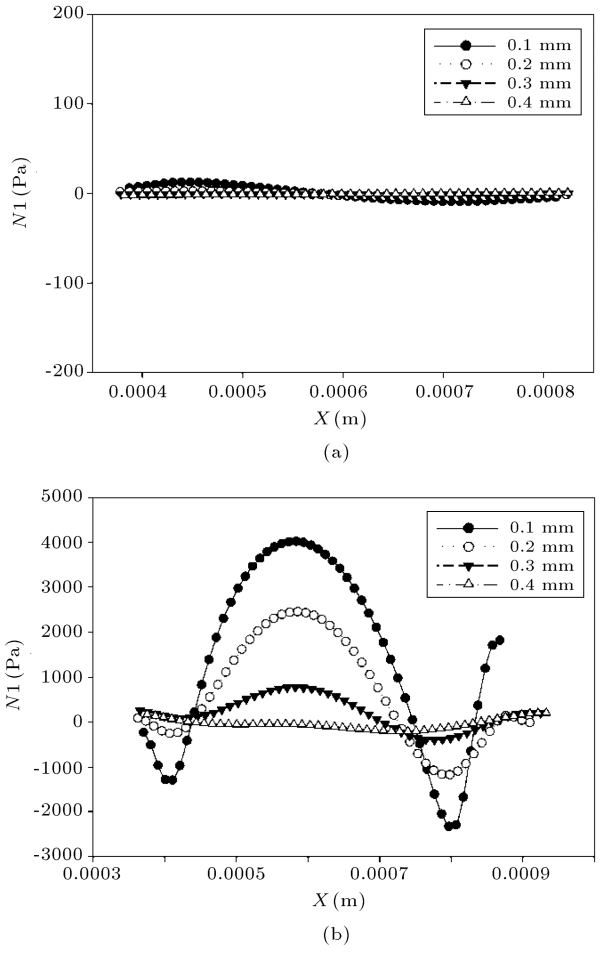

Figure 8. The first normal stress differences: (a) Newtonian fluid, and (b) viscoelastic fluid with the prescribed condition (P1.5r30).

die experienced higher stresses in the vicinity of the walls, it is expected that the fluid in that region show pronounced relaxation behavior which would reveal itself as velocity increases at the edges.

This was in compliance with the results obtained for the First Normal Stress Differences (FNSD) (Figure 8). It was shown that for Newtonian fluid, the FNSD was almost zero, whereas there was a considerable FNSD distribution for viscoelastic fluid. The FNSD in the vicinity of the die exit was the highest and as the extrudate went downward and the relaxation process proceeded, it started to vanish. It is also seen that the velocity increase at the outer edge is greater than that for the inner one, which could be attributed to the higher shear stress in the vicinity of the outer wall inside the die and higher local FNSD.

As the extrudate went down, the memory of the viscoelastic fluid faded out and the velocity profile started to become flat. Nevertheless, in spite of the Newtonian fluid, the viscoelastic fluid never reached complete fade-out state at the time span of the process. The comparison of the velocity profile of the Newtonian and viscoelastic fluid shows that the middle part of the velocity profile is similar in both types of fluid. It was expected that since the hydrodynamic stress was small in the middle part of the channel, no significant stresses were exerted on the fluid; hence, no significant elastic phenomena would be observed. However, as it was mentioned above, at the edges of extrudate, a significant difference could be seen, which was explained before.

By comparing the velocity profiles of the Newtonian and viscoelastic fluid in the extrudate (out of die), one may notice that the axial velocity of the viscoelastic fluid is lower than that of Newtonian fluid whose difference is much more pronounced at sections from the die outlet. This could be attributed to the shrinking back of the viscoelastic fluid due to its stress-relaxation.

4.3. Effect of operating conditions

4.3.1. Effect of flow rate/pressure of die

Figure 9 exhibits the velocity profile of viscoelastic fluid in the extrudate at different cross-sections for various flow rates. As it is well known, increasing the flow rate will increase the velocity magnitude which could be noticed in the result presented in Figure 9. Besides, it could increase the exerted stress on the fluid inside the die leading to the increase of the stored stress in the fluid and showing enhanced elastic effects. The predicted results for cross section (a) (Figure 9(a)) showed that at high flow rates, as depicted in Figure 10, due to higher extent of FNSD, the velocity profile showed more pronounced velocity difference across the section. However, the overall shape of the velocity profile remained the same for different flow rates.

As the extrudate went downward and polymer melt relaxed, the velocity profile flattened as explained above. But, for higher flow rates, fluid took more time to become relaxed and the velocity profile became completely flat, obvious in Figure 9.

In addition to the velocity profile, the extrudate profile was also affected by flow rate. As expected, increasing the flow rate increased the extrudate swell of the extrudate. Increasing the flow rate above 53% would cause an increase of 45% of the extrudate die-swell. Increasing the flow rate intensifies the exerted stress on the fluid leading to the increase of the extent of extrudate swell of the extrudate.

4.3.2. Effect of take-up velocity

Figure 11 presents the velocity profile of the fluid outside the die for different take-up velocities. The result showed that the take-up velocity do not have a significant effect on the velocity profile, especially in the vicinity of the die exit. At the section far from the die exit, the take-up velocity dominated the flow field and

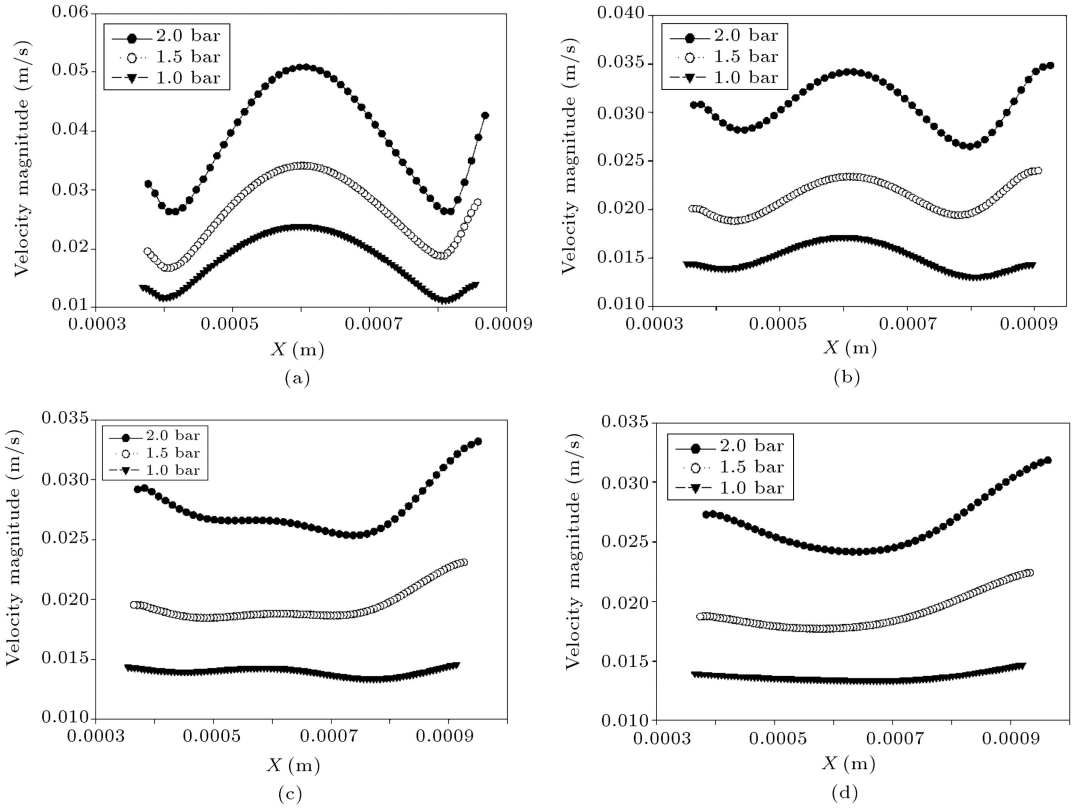

Figure 9. Velocity profile for viscoelastic fluid at the distance of (a) 0.1 mm, (b) 0.2 mm, (c) 0.3 mm, and (d) 0.4 mm at the extrudate at constant take-up velocity ($V = 0.204$ m/s).

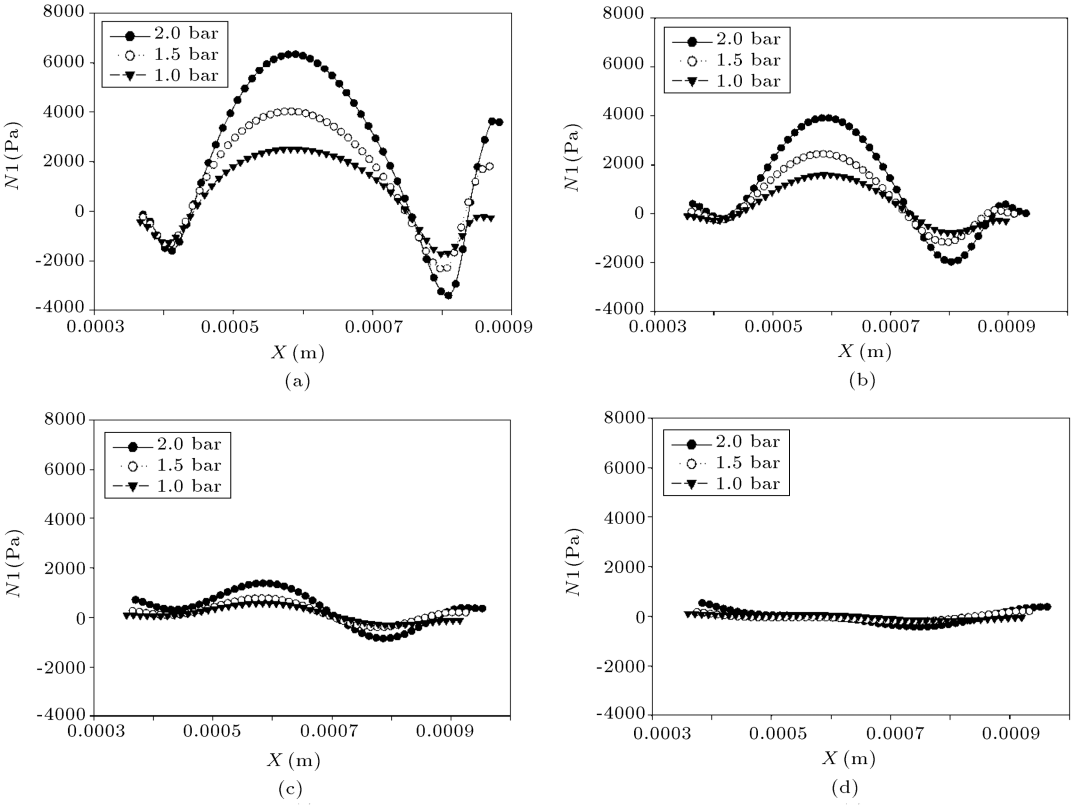

Figure 10. The FNSD for viscoelastic fluid at the distance of (a) 0.1 mm, (b) 0.2 mm, (c) 0.3 mm, and (d) 0.4 mm at the extrudate at constant take-up velocity ($V = 0.204$ m/s).

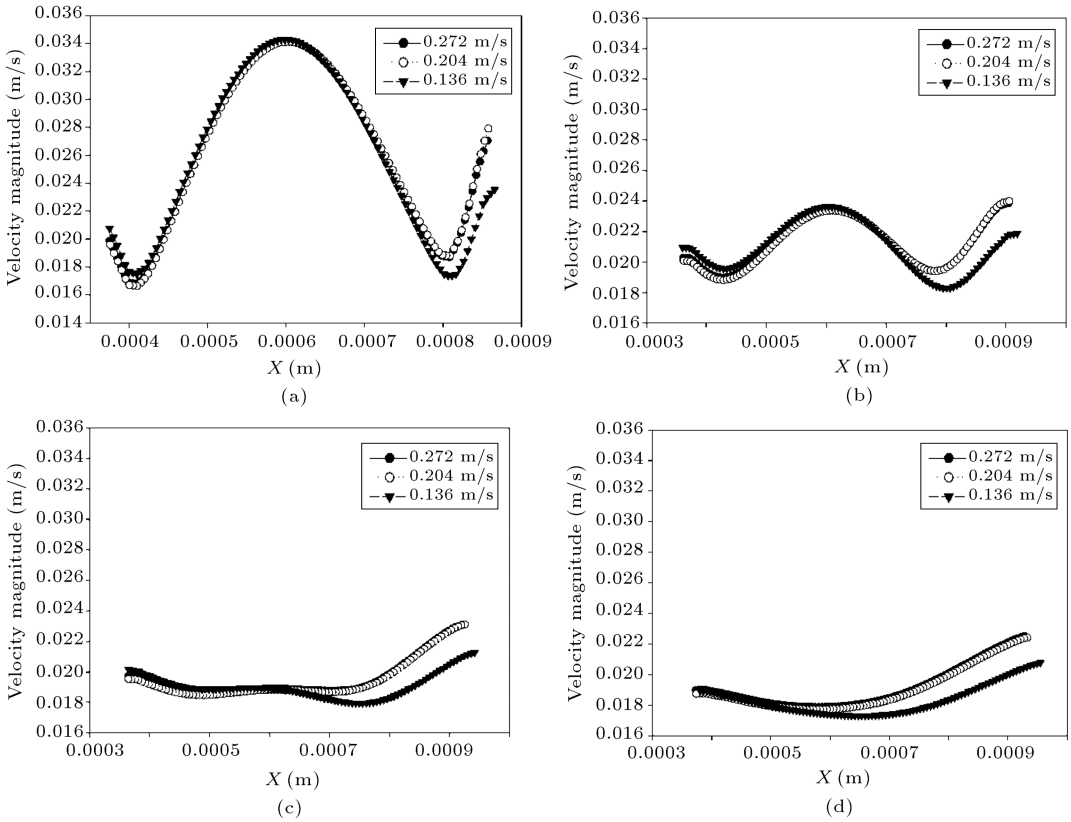

Figure 11. Velocity profile for viscoelastic fluid at the distance of (a) 0.1 mm, (b) 0.2 mm, (c) 0.3 mm, and (d) 0.4 mm at the extrudate at constant entrance pressure ($P = 1.5$ bar).

Table 3. The hollow fiber thickness at different operating conditions.

Take-up speed	Entrance pressure (bar)		
(m/s)	1	1.5	2
0.068	2.353 mm	—	—
0.136	1.661 mm	1.966 mm	—
0.204	1.353	1.638 mm	1.95 mm
0.272	—	1.415 mm	1.694 mm
0.34	—	—	1.512 mm

for higher take-up velocity, the velocity profiles were almost the same. However, at lower take-up velocity, the elastic response of the fluid was comparable to the take-up speed effect; hence, the effect was still noticeable.

The extrudate swell was affected by the take-up velocity, as expressed in Table 3. It was shown that the extent of extrudate swell decreased as the take-up velocity increased. Increasing the take-up velocity to about 100% would decrease the extrudate swell about 38%. It can be noticed that there was no linear relationship between the take-up velocity and the extrudate swell, as presented in Table 3.

The reason for this matter can be found in the fact that the fluid had damping effect which dissipates the excess stress exerted by the drawing device. As

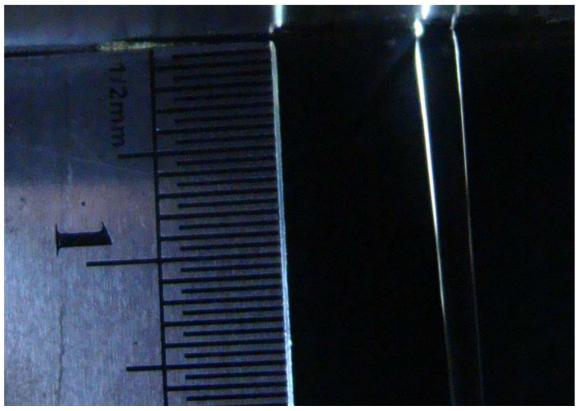

Figure 12. The image of the extrudate at entrance pressure of 2 bars and take-up velocity of 0.204 m/s.

take-up velocity increases, more stress dissipates and a certain amount of stress reaches the extrudate in the vicinity of the die. So, no linear relationship could be expected to be observed.

Then, at different flow rates and draw-up velocities, images were taken from the die exit. Photos were analyzed by Image J software. Figure 12 shows one of the images taken from die exit.

The extrudate profile was also investigated experimentally. For this purpose, the images of extrudate under different conditions, Figure 12, were analyzed

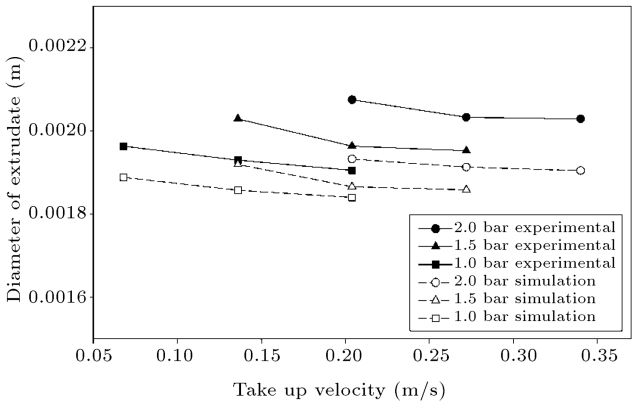

Figure 13. The comparison of the experimental results and simulation on extrudate swell.

using an open source image analyzing software, Image J, and results were compared to numerical ones.

5. Comparison with experimental data

Figure 13 depicts the comparison of experimental and simulation results of the simultaneous effects of flow rate and take-up speed on the extrudate swell. It shows that numerical results have the error of approximately 3% to 10% with respect to the experimental ones, showing good agreement between results. It should be pointed out that since Giesekus model and selected solving algorithm, DEVSS/SUPG, show a growing error as Weissenberg numbers increase, there may be an increasing error at higher flow rates, as can be seen in Figure 13.

6. Conclusion

The simulation of hollow fiber production process of a linear low-density polyethylene dope solution was performed using the finite-element method. To evaluate the effect of the fluid behavior, Newtonian and viscoelastic fluids were considered as the extrudate fluid. The viscoelastic fluid was assumed to obey Giesekus' model. The Discrete Elastic Viscous Split Stress (DEVSS) algorithm in cooperation with Streamline Upwind Petrov Galarkin (SUPG) approach was served as numerical scheme, and a Lagrangian grid front tracking method was employed to track the free surface of the extrudate. The results showed that the velocity profile in the vicinity of the die outlet indicated an up-turn pattern at the edge of the extrudate, while it was smoother for Newtonian fluid case. Also, it was shown that for Newtonian fluid, the first normal difference stress was almost negligible in comparison to viscoelastic one. According to the results, extrudate swell for viscoelastic fluid was much greater than that for Newtonian one. Moreover, the impact of operating condition, such as die back pressure and take-up velocity, was studied on the flow field and extrudate swell. Results showed that the velocity at extrudate increases with increasing back pressure. Increasing the back pressure by 53% would cause the extrudate die swell to increase by 45%. It was also depicted that the take-up velocity does not have a significant effect on the velocity profile, especially in the vicinity of the die exit. The extrudate swell of the extrudate was affected by the take-up velocity. Increasing the take-up speed to about 100% would decrease the extrudate swell by 38%. The extrudate profile was also investigated experimentally. The predicted results were compared with experimental observations showing that numerical results have the error of approximately 3% to 10% with respect to the experimental ones, indicating good agreement between the results.

Nomenclature

$\mathbf{D}$	Deformation rate tensor
$\mathbf{f}$	External force applied
G'	Storage moduli
G''	Loss moduli
$\mathbf{g}$	Gravitational acceleration
p	Pressure
$\mathbf{u}$	Velocity vector
α	Mobility factor
η_p	Zero shear viscosity of the fluid
λ	Relaxation time
ρ	Fluid density
$\boldsymbol{\tau}$	Stress tensor
$\boldsymbol{\tau}_{\mathbf{p}}$	Stress due to the elastic part
$\boldsymbol{\tau}_p^{\nabla}$	Upper convected derivative of the excess stress tensor
$\boldsymbol{\tau}_{\mathbf{s}}$	Stress due to the viscous part
ω	Angular frequency

References

1. Mok, S., Worsfold, D., Fouda, A. and Matsuura, T. "Surface modification of polyethersulfone hollow-fiber membranes by γ-ray irradiation", *J. Appl. Polym. Sci.*, **51**(1), pp. 193-199 (1994).
2. Feng, C.Y., Khulbe, K.C., Matsuura, T. and Ismail, A.F. "Recent progresses in polymeric hollow fiber membrane preparation, characterization and applications", *Sep. Purif. Technol.*, **111**(0), pp. 43-71 (2013).
3. Tanner, R. "A theory of die-swell", *J. of Polym. Sci., Part A-2: Polymer Physics*, **8**(12), pp. 2067-2078 (1970).
4. Pereira, C., Nobrega, R. and Borges, C. "Spinning process variables and polymer solution effects in the die-swell phenomenon during hollow fiber membranes

formation", *Braz. J. Chem. Eng.*, **17**(4-7), pp. 599-606 (2000).

5. Wang, D.-M. and Lai, J.-Y. "Recent advances in preparation and morphology control of polymeric membranes formed by nonsolvent induced phase separation", *Curr. Opin. Chem. Eng.*, **2**(2), pp. 229-237 (2013).
6. Batchelor, J., Berry, J. and Horsfall, F. "Die swell in elastic and viscous fluids", *Polym.*, **14**(7), pp. 297-299 (1973).
7. Orbey, N. and Dealy, J. "Isothermal swell of extrudate from annular dies; effects of die geometry, flow rate, and resin characteristics", *Polym. Eng. Sci.*, **24**(7), pp. 511-518 (1984).
8. Andrews, E. "Cooling of a spinning thread-line", *Br. J. Appl. Phys.*, **10**(1), p. 39 (1959).
9. Ziabicki, A. and Kedzierska, K. "Studies on the orientation phenomena by fiber formation from polymer melts. Part I. Preliminary investigations on polycapronamide", *J. Appl. Polym. Sci.*, **2**(4), pp. 14-23 (1959).
10. Denn, M.M., Petrie, C.J. and Avenas, P. "Mechanics of steady spinning of a viscoelastic liquid", *AIChE J.*, **21**(4), pp. 791-799 (1975).
11. Sano, Y. "Drying behavior of acetate filament in dry spinning", *Drying Technol.*, **19**(7), pp. 1335-1359 (2001).
12. Gou, Z. and McHugh, A.J. "Two-dimensional modeling of dry spinning of polymer fibers", *J. Non-Newtonian Fluid Mech.*, **118**(2), pp. 121-136 (2004).
13. Didari, H. "Simulation of die swell in hollow fiber's spinneret", Dissertation, Sahand University of Technology (2013).
14. Berghmans, S., Berghmans, H. and Meijer, H. "Spinning of hollow porous fibers via the TIPS mechanism", *J. Membr. Sci.*, **116**(2), pp. 171-189 (1996).
15. Beris, A.N. and Liu, B. "Time-dependent fiber spinning equations. 1. Analysis of the mathematical behavior", *J. Non-Newtonian Fluid Mech.*, **26**(3), pp. 341-361 (1988).
16. Lee, J.S., Jung, H.W., Kim, S.H. and Hyun, J.C. "Effect of fluid viscoelasticity on the draw resonance dynamics of melt spinning", *J. Non-Newtonian Fluid Mech.*, **99**(2), pp.159-166 (2001).
17. Joo, Y., Sun, J., Smith, M., Armstrong, R., Brown, R. and Ross, R. "Two-dimensional numerical analysis of non-isothermal melt spinning with and without phase transition", *J. Non-Newtonian Fluid Mech.*, **102**(1), pp. 37-70 (2002).
18. Behzadfar, E., Ansari, M., Konaganti, V.K. and Hatzikiriakos, S.G. "Extrudate swell of HDPE melts: I. Experimental", *J. Non-Newtonian Fluid Mech.*, **225**, pp. 86-93 (2015).
19. Konaganti, V.K., Ansari, M., Mitsoulis, E. and Hatzikiriakos, S.G. "Extrudate swell of a high-density polyethylene melt: II. Modeling using integral and differential constitutive equations", *J. Non-Newtonian Fluid Mech.*, **225**, pp. 94-105 (2015).
20. Konaganti, V.K., Ansari, M., Mitsoulis, E. and Hatzikiriakos, S.G. "The effect of damping function on extrudate swell", *J. Non-Newtonian Fluid Mech.*, **236**, pp. 73-82 (2016).
21. Konaganti, V., Behzadfar, E., Ansari, M., Mitsoulis, E. and Hatzikiriakos, S. "Extrudate swell of high density polyethylenes in slit (flat) dies", *Int. Polym. Proc.*, **31**(2), pp. 262-272 (2016).
22. Baaijens, F.P., Selen, S.H., Baaijens, H.P., Peters, G.W. and Meijer, H.E. "Viscoelastic flow past a confined cylinder of a low density polyethylene melt", *J. Non-Newtonian Fluid Mech.*, **68**(2), pp. 173-203 (1997).
23. Soulaïmani, A., Fortin, M., Dhatt, G. and Ouellet, Y. "Finite element simulation of two-and three-dimensional free surface flows", *Comput. Methods in Appl. Mech. Eng.*, **86**(3), pp. 265-296 (1991).
24. Calin, A., Wilhelm, M. and Balan, C. "Determination of the non-linear parameter (mobility factor) of the Giesekus constitutive model using LAOS procedure", *J. Non-Newtonian Fluid Mech.*, **165**(23), pp. 1564-1577 (2010).
25. Tian, H., Zhao, D., Wang, M., Jin, G. and Jin, Y. "Study on extrudate swell of polypropylene in double-lumen micro profile extrusion", *J. Mater. Process. Technol.*, **225**, pp. 357-368 (2015).
26. Yesilata, B., Clasen, C. and McKinley, G.H. "Nonlinear shear and extensional flow dynamics of wormlike surfactant solutions", *J. Non-Newtonian Fluid Mech.*, **133**, pp. 73-90 (2006).
27. Giesekus, H. "A simple constitutive equation for polymer fluids based on the concept of deformation-dependent tensorial mobility", *J. Non-Newtonian Fluid Mech.*, **11**(1-2), pp. 69-109 (1982).

Biographies

Hamid Didari received his BSc and MS degrees in Chemical Engineering from Sahand University of Technology, Iran, in 2010 and 2013, respectively. His field of study is Modeling and Simulation in Fluid Mechanic. He entered the Tabriz University as a PhD student in 2014.

Mahdi Salami Hosseini obtained his BSc and MSc degrees from Amirkabir University of Technology in 2001 and 2004, respectively. He received his PhD from Amirkabir University of Technology in Polymer Engineering in 2009. He joined Polymer Engineering Department at Sahand University of Technology as an Assistant Professor in 2009 and became an Associate Professor in 2015. His current research interests

include process simulation and numerical rheology using Finite-Element Method (FEM) and Stokesian Dynamics (SD) focusing on microfluidic devices.

Reza Yegani is currently a scientific member of Sahand University of Technology, Tabriz, Iran. He received his BSc degree in Chemical Engineering from Sahand University of Technology and MSc degree from Amirkabir University of Technology. He graduated from Kobe University of Japan in 2005 and has collaborated in Renaissance Energy Research Co. in Japan as a post-doctoral researcher up to 2008. He established the first Membrane Technology Research Center in Sahand University of Technology.